

Utah State University

DigitalCommons@USU

Reports

Utah Water Research Laboratory

January 1969

The Effect of Sediment Properties of an Ultrasonic Plane Wave

G. H. Flammer

N. E. Stauffer Jr.

E. Y. Liu

Follow this and additional works at: https://digitalcommons.usu.edu/water_rep



Part of the [Civil and Environmental Engineering Commons](#), and the [Water Resource Management Commons](#)

Recommended Citation

Flammer, G. H.; Stauffer Jr., N. E.; and Liu, E. Y., "The Effect of Sediment Properties of an Ultrasonic Plane Wave" (1969). *Reports*. Paper 481.

https://digitalcommons.usu.edu/water_rep/481

This Report is brought to you for free and open access by the Utah Water Research Laboratory at DigitalCommons@USU. It has been accepted for inclusion in Reports by an authorized administrator of DigitalCommons@USU. For more information, please contact digitalcommons@usu.edu.



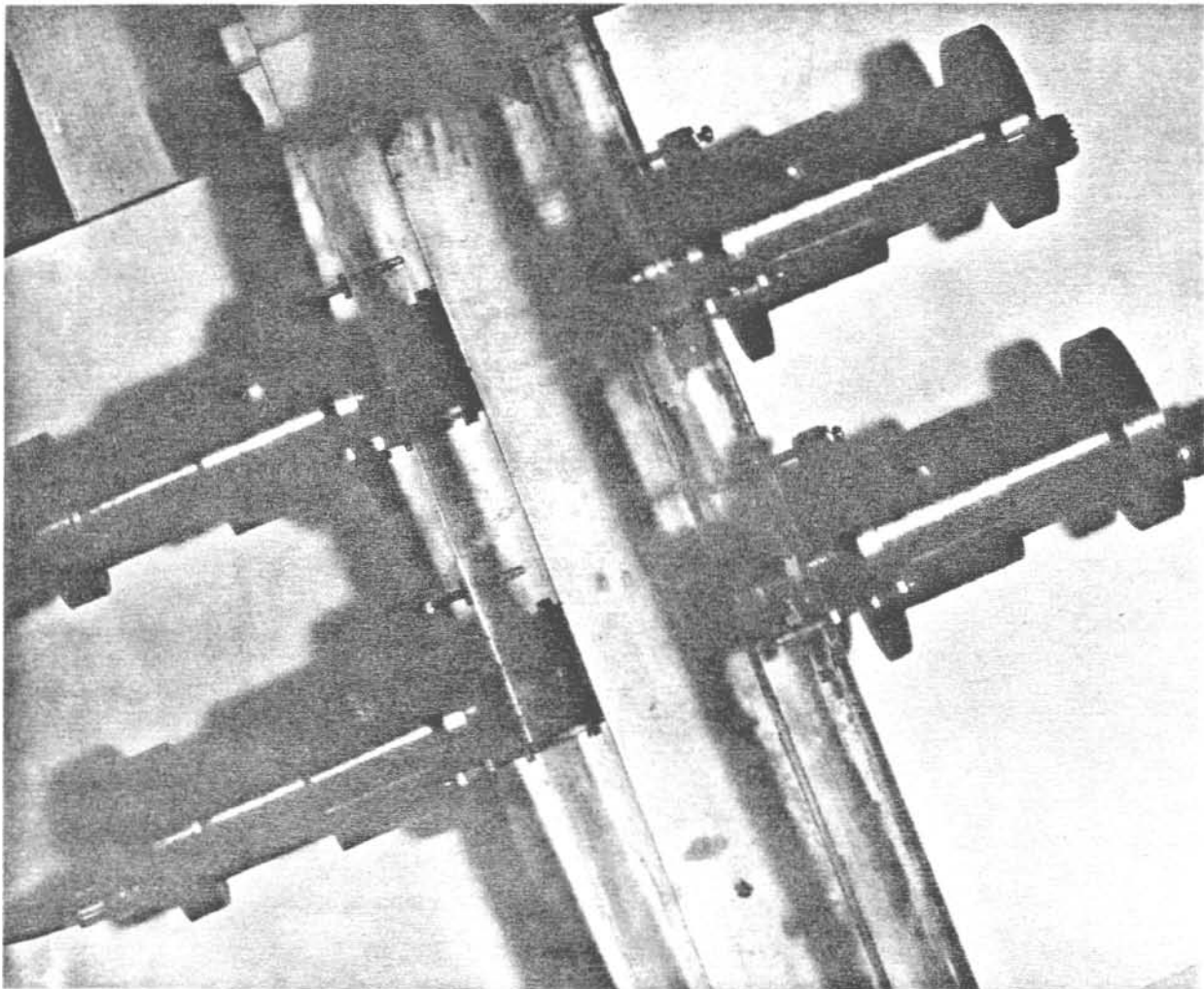


Logan, Utah 84321

Absorption

The Effect of Sediment Properties of an Ultrasonic Plane Wave

*Utah Water Research Laboratory / College of Engineering
by G. H. Flammer, N. E. Stauffer, Jr., and E. Y. Liu
September 1969*



THE EFFECT OF SEDIMENT PROPERTIES ON THE ATTENUATION
OF AN ULTRASONIC PLANE WAVE

by

G. H. Flammer, N. E. Stauffer, Jr., and E. Y. Liu

801-750-2863
2775

Utah Water Research Laboratory
College of Engineering
Utah State University

September 1969

PREC30-1

THE EFFECT OF SEDIMENT PROPERTIES ON THE ATTENUATION OF AN ULTRASONIC PLANE WAVE

Synopsis

Experimental results of the attenuation of an ultrasonic plane wave by monodisperse suspensions of sediments are presented for a variety of sediment properties. The results are compared with the theoretical equations over the viscous, the scattering, the transition, and the diffraction loss ranges. Significant differences between theory and experiment are shown. In some cases the theoretical equations are improved; whereas in other cases the disparity between theory and experiment is so great that both equations are given for comparison. Experiments were made in water using particles of specific gravity greater than 2.0.

TABLE OF CONTENTS

Introduction	1
Theory	1
Experimental Results	2
Viscous loss range	3
Scattering loss range	5
Diffraction loss range	6
Transition loss range	11
Conclusions	14
Literature Cited	14

LIST OF FIGURES

Figure		Page
1	Nondimensional plot of the theoretical equation, empirical equation, and experimental data in the viscous loss range with $fd^2/v = 500$ and $C = 1000$ ppm by volume	4
2	Comparison of experimental scattering loss curves with theoretical scattering and diffraction loss curves with density ratio as parameter. $C = 1000$ ppm by volume and $C_s = 1.5$	7
3	Comparison of the true scattering loss curves (i.e. with viscous attenuation subtracted out) with theoretical curves. $C = 1000$ ppm by volume	8
4	Scattering loss range experimental data. $C = 1000$ ppm by volume. (o-experimental data for natural sands.)	9
5	Transition loss curves for quartz sands of various shape factors. $C = 1000$ ppm by volume. (o- $C_s = 1.45$, o- $C_s = 1.55$, + $C_s = 1.65$.)12
6	Dimensionless attenuation of two metal powders covering part or all of the diffraction, transition, scattering and viscous loss ranges. Concentration = 1000 ppm by volume. (o-Tungsten $S_g = 18.9$, + Silicon $S_g = 2.4$.)13

LIST OF TABLES

Table		Page
1	Sediments tested in the viscous loss range and their pertinent properties	5
2	Sediments tested in the scattering loss range and their properties10
3	Sediments tested in the diffraction loss range and their average shape factor10

THE EFFECT OF SEDIMENT PROPERTIES ON THE ATTENUATION OF AN ULTRASONIC PLANE WAVE

Introduction

Previous studies of the attenuation of an ultrasonic plane wave passing through a monodisperse sediment suspension have been primarily theoretical with limited experimental verification. Because of the complexity of the problem, simplifying assumptions have been necessary in the derivations. This study stresses the use of experimental results to verify or improve existing theoretical expressions and to point the way to future theoretical studies.

Theory

The basic relation for the additional energy loss of an ultrasonic plane wave due to the presence of suspended sediments in the fluid media is

$$E = E_0 e^{-\alpha x} \quad \dots \quad (1)$$

where

- E is the sound energy flux at a given point with sediment present in the transmitting media,
- E₀ is the sound energy flux at the same point if no sediment were present,
- e is the base of the Napierian Logarithm,
- α is the attenuation coefficient due to the sediment alone in decibels per centimeter, and
- x is the distance from the sound source to the point of measurement.

The attenuation coefficient, α, is made up of three loss mechanisms. The first of these is due to shear waves set up at the liquid-solid interface when the particle vibrates in response to the sound wave but lags it. The range where these shear waves predominate the sound wave attenuation is called the "viscous loss range." The second loss mechanism arises from the scattering of energy from the sound path due to a reradiation by the particle of the incident plane wave. The pattern and intensity of the reradiated wave are functions of the ratio of the sound wave length, λ, to the particle circumference, 2πr. For λ >> 2πr the reradiated wave spreads out more or less uniformly in all directions. This range has been called the "scattering loss range." As λ approaches 2πr, the scattering pattern becomes more complicated and changes rapidly as the frequency changes. The writers have named this region "the transition loss range" because it is situated between two very different, but stable, radiation patterns. For λ >> 2πr, half of the scattered wave is concentrated straightforward, thus interfering with the incident wave and causing the sediment particle to cast a shadow. The other half of the scattered wave is spread out uniformly over all directions. This region is the "diffraction loss range." The third loss mechanism is due to heat conduction down thermal gradients. It is significant only when the suspending media or suspended particle is compressible.

Several theoretical studies have been made to determine the attenuation coefficient for uniform size suspensions. Lord Rayleigh (1945), Sewell (1910), Epstein (1941), Lamb (1945), Urick (1948), Carhart (1950), and Vigoureux (1950), have derived mathematical expressions for α when $\lambda \gg 2\pi r$. Thus, they studied either the viscous loss range or the scattering loss range or both. Weinel (1953) showed that for rigid particles in water, the results of Urick, Epstein, and Carhart are identical for the viscous loss range. Urick and Sewell's expression for the scattering loss range are special cases of Lamb's more general expression. Anderson (1950) and Farn (1951) studied the transition loss region. They found that in this range the particles are elastic and cannot be assumed to be rigid. Morse (1948) derived an expression for the attenuation coefficient α for the diffraction loss range, i.e. where $\lambda \gg 2\pi r$.

Simplifying assumptions have been necessary to solve the complex relations. The first assumption generally made is that the particles are rigid spheres. Anderson showed that for particles in water having a specific gravity greater than 2.0 and a sound velocity greater than twice that of water, that the particles may be considered rigid for $2\pi r/\lambda$ greater than 3.0 and less than 0.5. The transition from the scattering loss to the diffraction loss ranges includes this region and it has been called by the authors "the transition loss range." The second assumption is that the particles are far enough apart so they do not interfere with each other. This assumption has been proven valid up to concentrations as high as 20 percent by volume.

Several experimental investigations have been made covering one or more of these loss ranges. Urick's work was in the viscous loss range. Stakutis, et al. (1955), and Busby and Richardson (1955) partly covered both the viscous and scattering loss ranges. Killen (1956) covered the diffraction loss region and Flammer (1958) covered both the transition and diffraction loss ranges. Stauffer (1964) covered all four ranges. Liu (1965) studied the diffraction and transition loss ranges using natural sands.

The experimental results of some cases do not agree with theory. Undoubtedly, this is due to the simplifying assumptions and failure to include pertinent variables in the theoretical studies. The lack of agreement between theory and experiment prompted this study. A National Science Foundation grant supplied the necessary financial support.

Experimental Results

The experimental equipment was a standard pulse system using matched transmitting and receiving x-cut quartz crystals. The frequency range was from 1.5 to 55 mcs. The ultrasonic path length was 2 inches across a recirculating vertical chamber.

In order to simplify plotting, dimensional analysis was used to reduce the number of variables. The general attenuation coefficient may be expressed as

$$\alpha = \phi(C, d, \lambda, \rho, \rho_0, \nu, \beta_1, \beta_0, \sigma, C_s) \quad \dots \quad (2)$$

where

- C is the concentration in parts per million by volume,
- d is the particle diameter,

mega

λ is the sound wave length,
 ρ and ρ_0 are the densities of the particles and fluid respectively,
 ν is the kinematic viscosity of the fluid,
 β_1 and β_0 are the bulk moduli of the particle and fluid respectively,
 σ is Poisson's ratio of the particle, and
 C_s is the shape factor.

The shape factor is defined as $C_s = L_1/L_2$ where L_1 is the longest axis and L_2 is the mean diameter of the particle normal to the longest axis. This ratio was obtained by averaging the measurements from projections of microphotographs containing approximately 50 particles each. The two-dimensional measurements assumed that the particles were rounded normal to the longest axis which was reasonably true for the sediments studied.

Water was the suspending fluid and all sediments had specific gravities greater than 2.0. Certain of the theoretical equations were chosen for comparison with experimental results based on the assumptions made in their derivation.

Viscous loss range. Urlick's expression for this range is,

$$\alpha = \frac{CKS(\gamma-1)^2}{S^2 + (\gamma + \tau)^2} \times 8.68 \text{ db/cm} \quad \dots \quad (3)$$

where $K = 2\pi/\lambda$, $\gamma = \rho/\rho_0$, $S = [9/(2Bd)] [1 + 2/(Bd)]$, $B = [w/(2\nu)]^{1/2}$, $w = 2\pi f$, f is the frequency, and $\tau = 1/2 + 9/(2Bd)$. Other symbols are as previously defined.

For the viscous loss range

$$\alpha = \phi(C, \lambda, \rho, \rho_0, \nu, d, C_s) \quad \dots \quad (4)$$

For all ranges α is a linear first order function of C so that the concentration need not be further considered. The size fractions in this range were obtained by sedimentation methods which inherently give an equivalent spherical size; therefore, shape factor was ignored. By Buckingham's Pi Theorem

$$\alpha\lambda = \phi_1 \left(\frac{fd^2}{\nu}, \rho/\rho_0 \right) \quad \dots \quad (4a)$$

thus $\alpha\lambda$ is a function of a Reynolds number and the relative density.

Five metal powders were tested in this range as shown on Table 1. Fig. 1 shows the experimental results. The equation fitting these points is

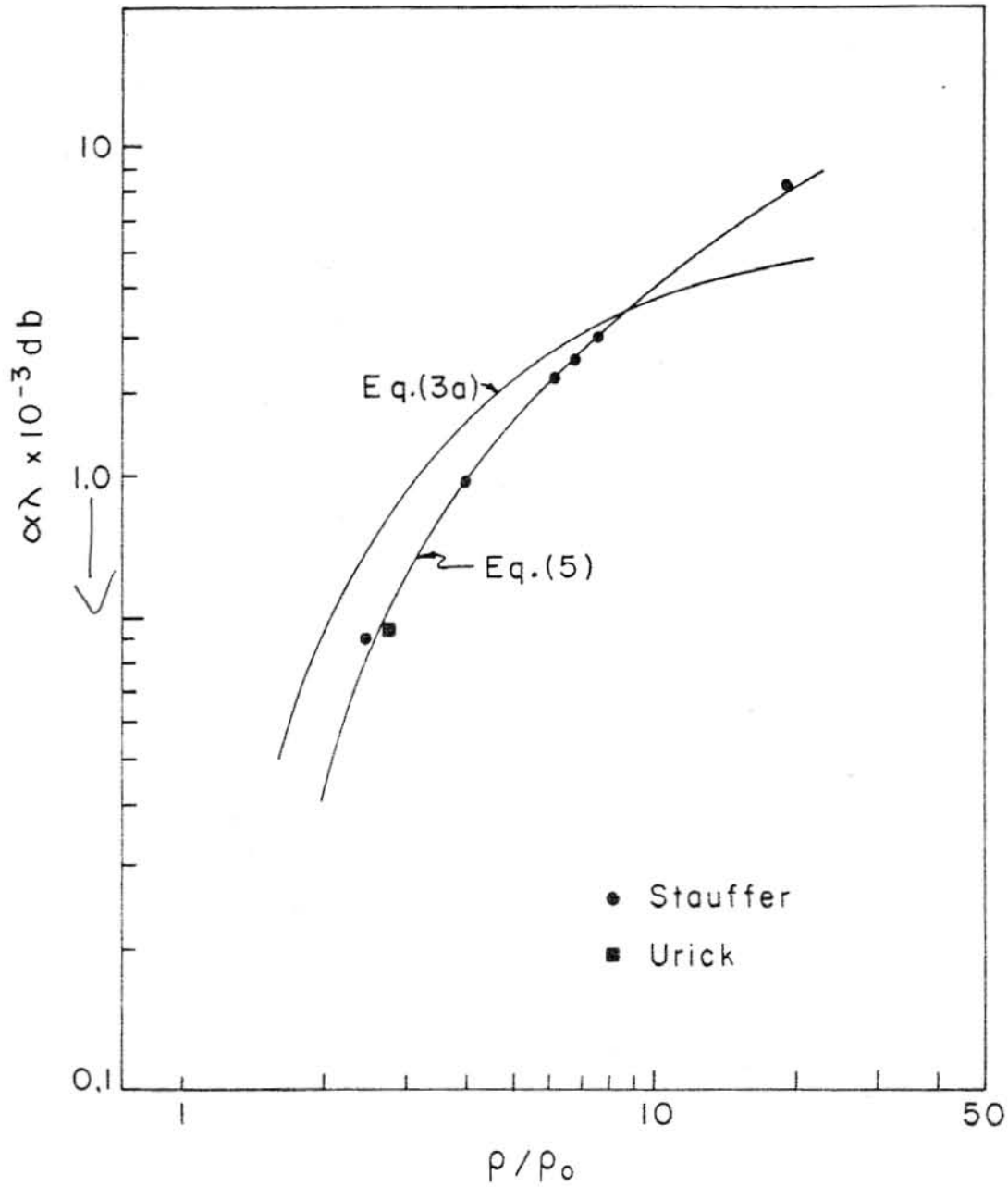


Fig. 1. Nondimensional plot of the theoretical equation, empirical equation, and experimental data in the viscous loss range with $fd^2/\nu = 500$ and $C = 1000$ ppm by volume.

Table 1. Sediments tested in the viscous loss range and their pertinent properties.

Sediment	Specific Gravity
silicon	2.4
antimony	6.6
tin	7.2
molybdenum	9.6
tungsten	19.0

$$\alpha \lambda = 22.5 C \left(\frac{fd^2}{\nu} \right)^{1/2} \left(\ln \frac{\rho}{\rho_o} \right)^2 \text{ decibels} \quad \dots \quad (5)$$

Comparing this equation with Urick's equation expressed in nondimensional form shows the equations to be similar if the log term is expanded in an infinite series. Urick's equation includes a term which approximates the first term of the infinite series. For the range of data taken, $S^2 < 0.065$ and $1/\beta r < 0.1$, simplifies his equation as follows:

$$\alpha \lambda = 138 C \left(\frac{fd^2}{\nu} \right)^{-1/2} \left(\frac{\rho/\rho_o - 1}{\rho/\rho_o + 1/2} \right)^2 \quad \dots \quad (3a)$$

Eq. 5 with the log term expanded is

$$\alpha \lambda = 90 C \left(\frac{fd^2}{\nu} \right)^{-1/2} \left[\left(\frac{\rho/\rho_o - 1}{\rho/\rho_o + 1} \right)^2 + \frac{2}{3} \left(\frac{\rho/\rho_o - 1}{\rho/\rho_o + 1} \right)^4 + \dots \right] \quad \dots \quad (5a)$$

Fig. 1 shows that Eq. 5a fits the data much better than Urick's equation.

Scattering loss range. Lamb's expression for the scattering loss range is

$$\alpha = 1.08 \left[1/3 \left(\frac{\rho - \rho_o}{2\rho + \rho_o} \right)^2 \right] CK^4 d^3 \text{ db/cm} \quad \dots \quad (6)$$

For this range the following variables are considered

$$\alpha = \phi(C, d, \lambda, \rho, \rho_o, C_s) \quad \dots \quad (7)$$

which reduces in dimensionless terms to

$$\alpha\lambda = \phi_2 (\pi d/\lambda, C, \rho, \rho_o, C_s) \quad \dots \quad (7a)$$

Eq. 6 in nondimensional form is

$$\alpha\lambda = 54.5 \left[1/3 + 1/4 \left(\frac{\rho/\rho_o - 1}{\rho/\rho_o + 1/2} \right)^2 \right] \frac{\pi d}{\lambda}^3 C \quad \dots \quad (6a)$$

Twelve sediments were tested in the scattering loss ranges as listed with their pertinent properties in Table 2. The resulting empirical equation is

$$\alpha\lambda = 6.68 C (\rho/\rho_o)^{1/2} \left(\frac{\pi d}{\lambda} \right)^{\frac{1.74}{\sqrt[3]{\rho/\rho_o}}} C_s^{-1.28} \quad \dots \quad (8)$$

This equation is plotted on Fig. 2. Eqs. 6a and 8 are not comparable since Eq. 8 actually is for an apparent scattering loss—i.e., it includes viscous loss with the scattering loss and Eq. 6a does not. In order to compare the results, the viscous loss was subtracted from Eq. 8 and the results compared with Eq. 6a on Fig. 3. The slopes of the curves are the same, but the intercepts are shifted. Liu found the equation for the natural sands tested by Stauffer to be

$$\alpha\lambda = 11.37 C \left(\frac{\pi d}{\lambda} \right)^{1.15} C_s^{-2.0} \quad \dots \quad (9)$$

For these sands $S_g \approx 2.65$. Fig. 4 shows Eq. 9 and the experimental data.

Diffraction loss range. Morse's expression for the diffraction loss range is

$$\alpha = 13.03 \frac{C}{d} \quad \dots \quad (10)$$

The attenuation is a function of

$$\alpha = \phi (C, d, \lambda, C_s) \quad \dots \quad (11)$$

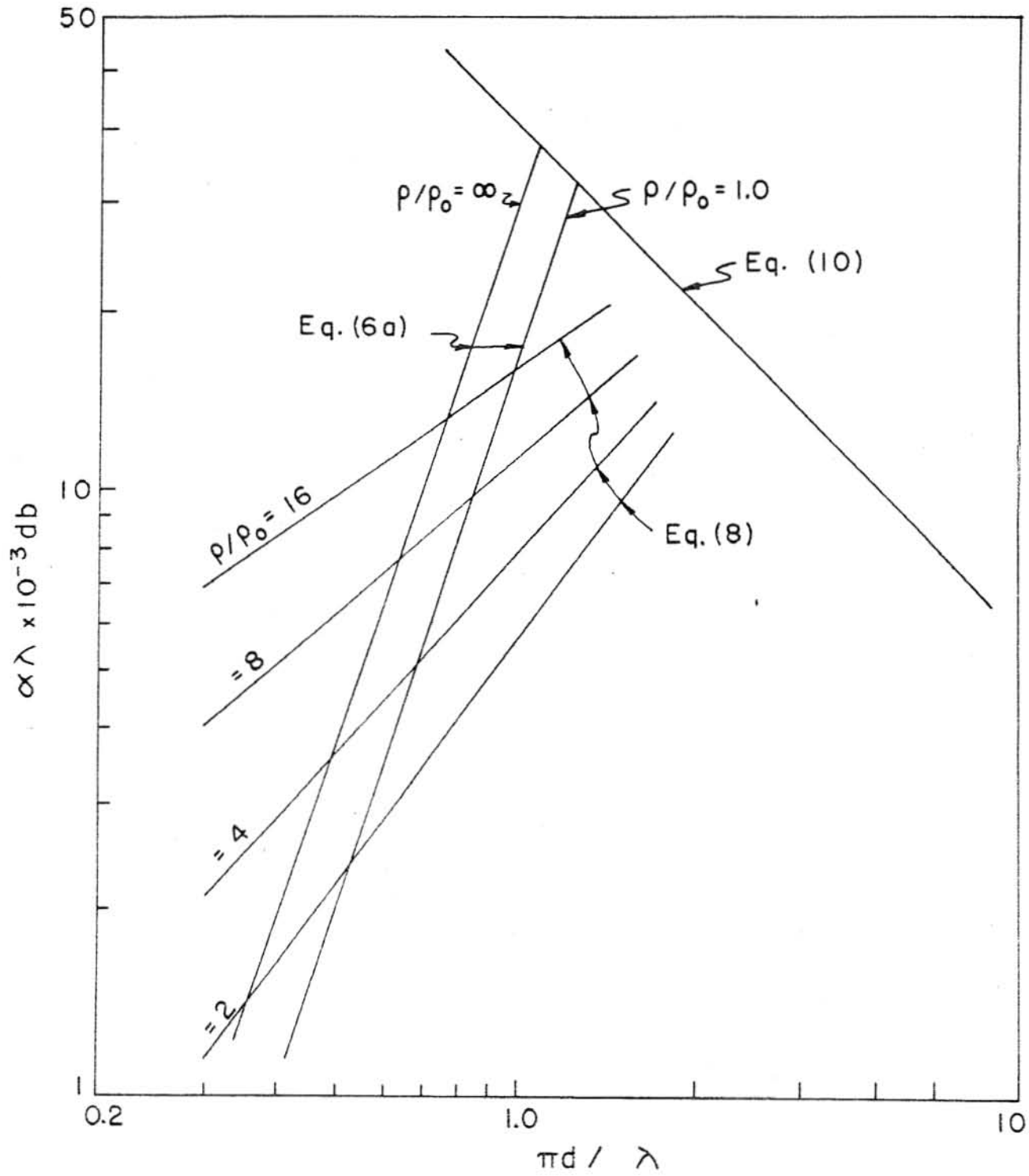


Fig. 2. Comparison of experimental scattering loss curves with theoretical scattering and diffraction loss curves with density ratio as parameter. $C = 1000$ ppm by volume and $C_s = 1.5$.

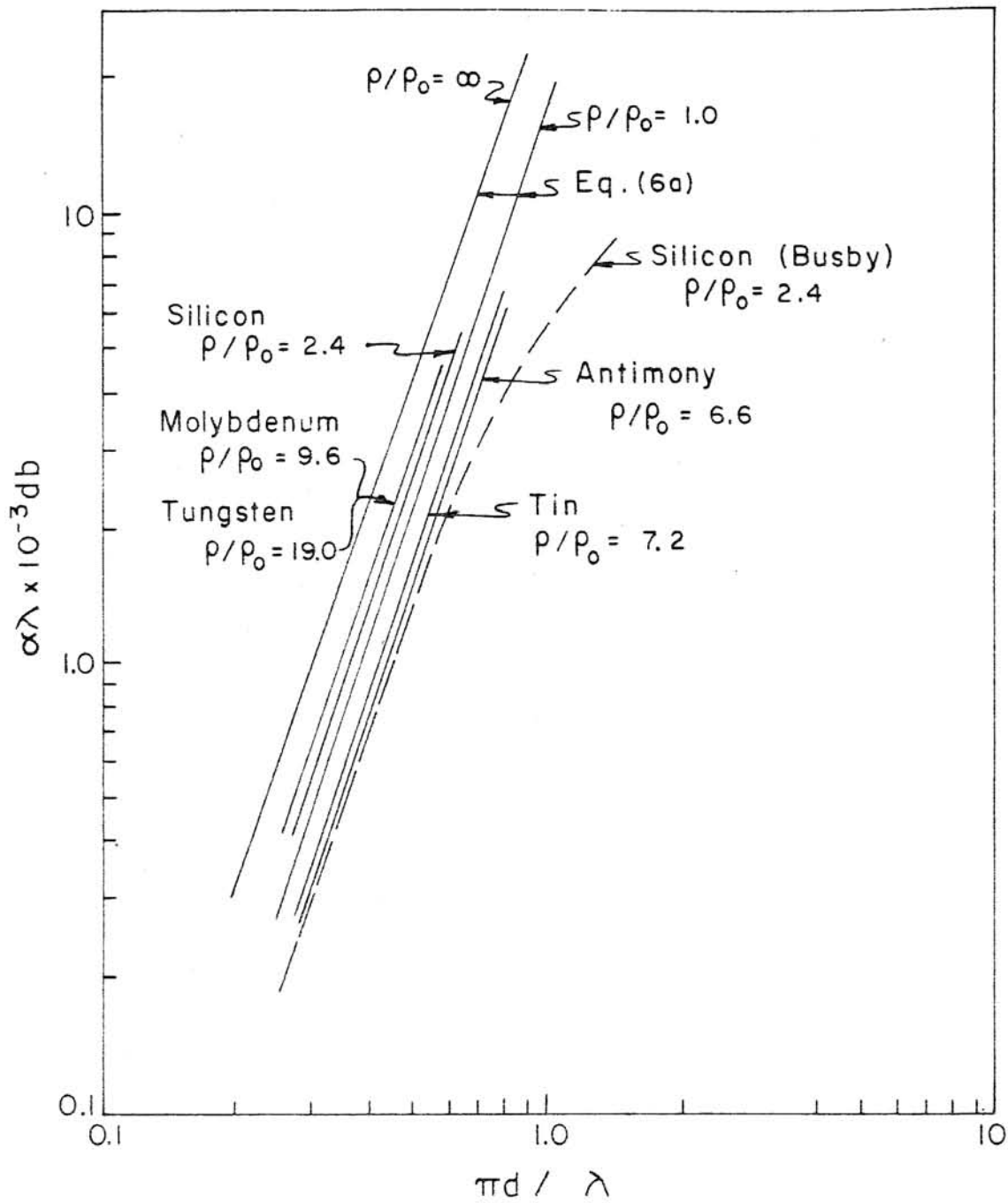


Fig. 3. Comparison of the true scattering loss curves (i.e. with viscous attenuation subtracted out) with theoretical curves. $C = 1000$ ppm by volume.

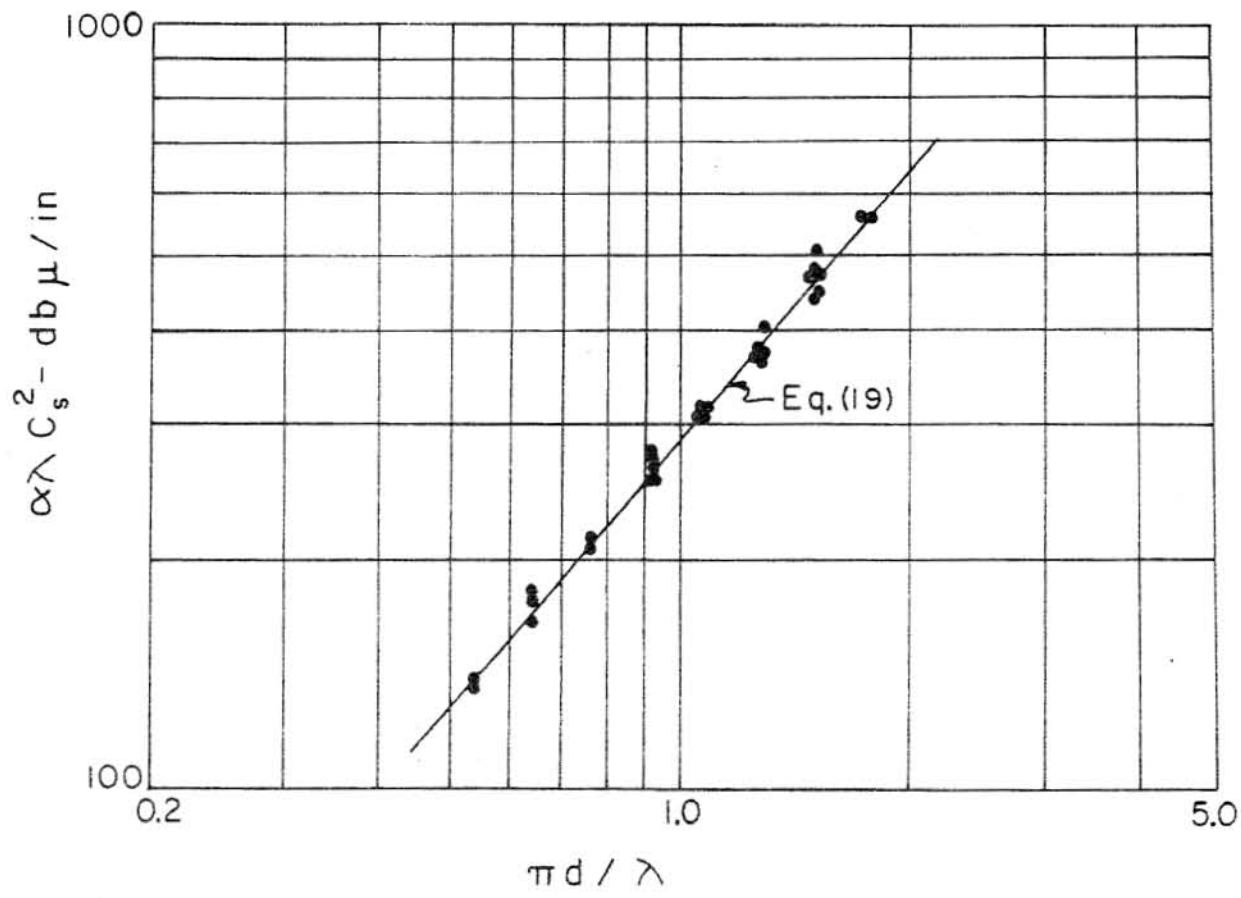


Fig. 4. Scattering loss range experimental data. C = 1000 ppm by volume. (o-experimental data for natural sands.)

Table 2. Sediments tested in the scattering loss range and their properties.

Sediment	Specific gravity	Average shape factor
Tungsten	19.0	1.97
Molybdenum	9.6	1.80
Cobalt	8.7	1.75
Tin	7.2	2.05
Zinc	7.1	1.96
Antimony	6.6	1.90
Aluminum Oxide	3.9	1.76
Silicon Carbide	3.2	1.77
Aluminum	2.7	1.88
Glass beads	2.5	1.00
Silicon	2.4	1.80
Pumice	2.2	2.30

Table 3. Sediments tested in the diffraction loss range and their average shape factor.

Sediment	Average shape factor*
Silicon	1.80
Zinc	2.00
Molybdenum	1.90
Pumice	2.10
Aluminum Oxide	1.75
South Fork White River Sand	1.45
Pigeon Roost Creek Sand	1.58
Fort Collins White Sand	1.60
Fort Collins River Sand	1.65
Minnesota Silica Sand	1.56
Arches Monument Sand	1.63
Missouri River Sand	1.70
Kansas River Sand	1.65
Loup River Sand	1.55
Kiowa Creek Sand	1.70
Elkhorn River Sand	1.50
Mississippi River Sand	1.42
Glass Beads	1.00

*Stauffer used an average shape factor for the entire size distribution. Liu used the shape factor for each size fraction, which improved his results considerably.

which reduces in dimensionless form to

$$\alpha\lambda = \left(\frac{\pi d}{\lambda}, C, C_s \right) \dots \dots \dots (12)$$

Eq. 11 in nondimensional form is

$$\alpha\lambda = 40.80 C \left(\frac{\pi d}{\lambda} \right)^{-1.0} \dots \dots \dots (13)$$

Eighteen sediments were tested in this range as given in Table 3, along with their respective average shape factors. Five of these sediments were metal powders, twelve were natural sediments, and one was glass beads. The resulting empirical equation is

$$\alpha\lambda = 11.28 C \left(\frac{\pi d}{\lambda} \right)^{-0.9} C_s^{1.9} \dots \dots \dots (14)$$

Liu improved this equation by defining the diffraction range as $(\pi d)/\lambda > 12.5$. Stauffer used $(\pi d)/\lambda > 3.0$; however, the data begins to curve below $(\pi d)/\lambda = 12.5$. Liu's equation for quartz sands is

$$\alpha\lambda = 16.41 C C_s^{1.7} \left(\frac{\pi d}{\lambda} \right)^{-1.0} \dots \dots \dots (15)$$

The power of the diameter agrees with theory.

Transition loss range. The theoretical equation for this range involves infinite series, so no attempt was made to find an empirical relation. However, the curves for the twelve quartz sands covering three different shape factors are shown in Fig. 5.

According to theory, the elastic properties of the particles become important in this range, but these properties are essentially constant for the natural sediments tested.

Since the density, shape factor, bulk modulus, and Poisson ratio are all important for the transition loss range, it wasn't possible to separate out the respective effects; however, a few observations can be made. The slope of the curve for the diffraction range is a constant; whereas for the scattering loss range, it is a function of the relative density of the particle. Since the transition curve joins these two ranges, its shape is obviously a function of the relative density. In fact, any variables in either Eq. 8 or 15 affect the shape of the transition curve. Insufficient data were available to define the effects of the elastic properties. These properties enter into the theoretical equations in complicated infinite series. Furthermore, the size fractions used were not monodisperse but had a finite spread of sizes which tended to mask the unique scattering pattern and attenuation properties of the individual particle. Fig. 6 shows two metal powders tested over all four ranges. The reason for the excessive scatter for $\pi d/\lambda < 1.0$ is that the viscous loss becomes increasingly important

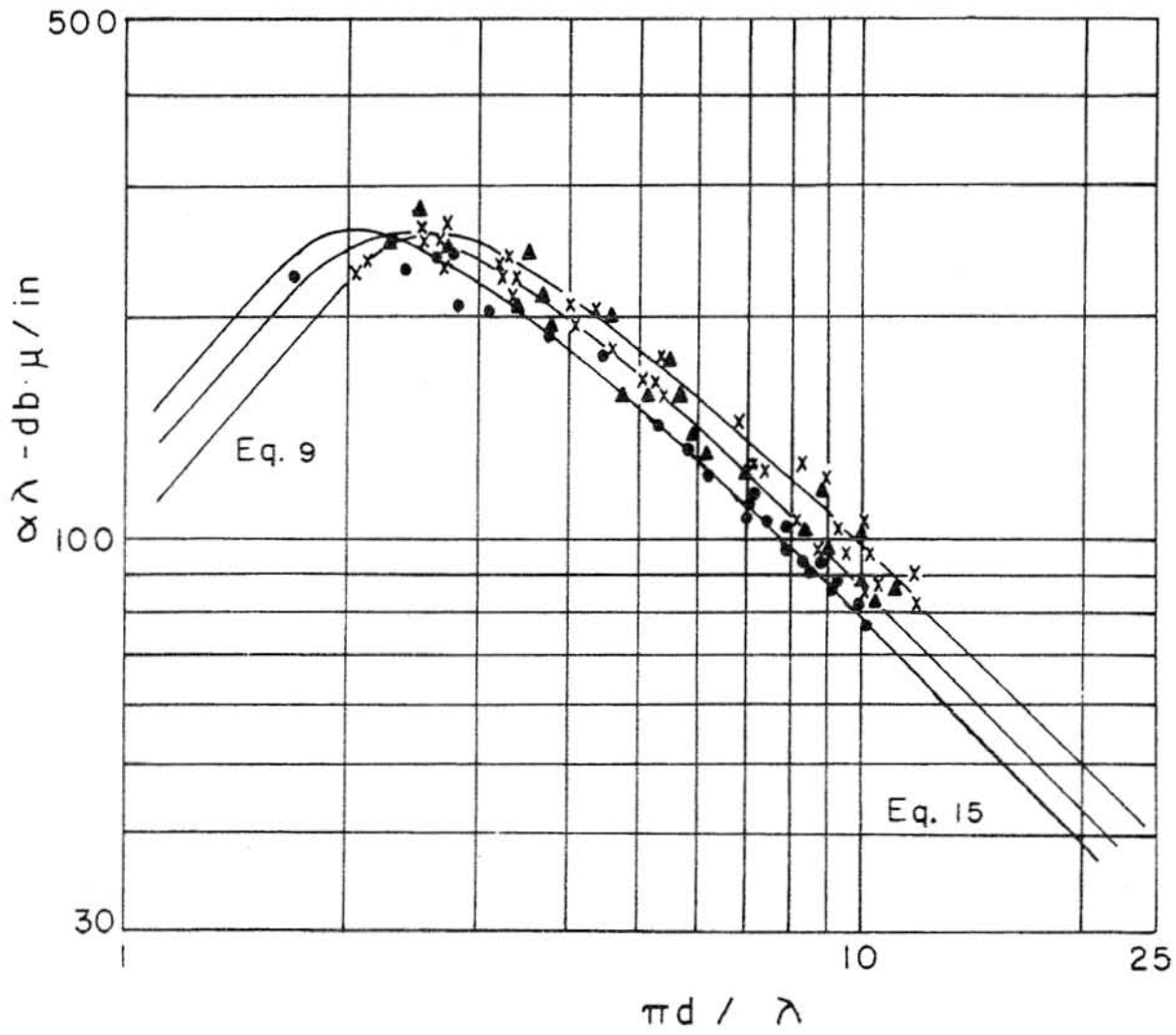
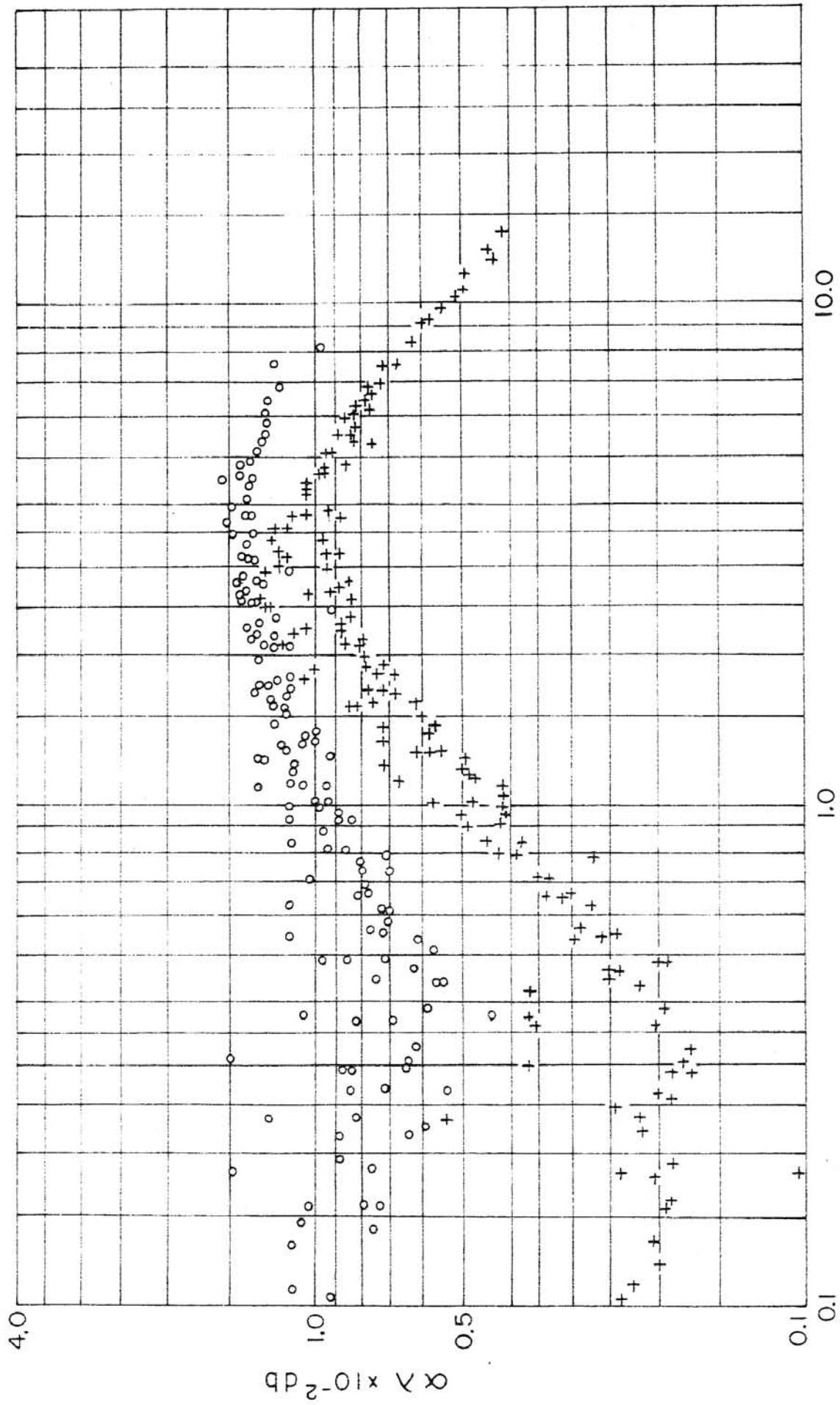


Fig. 5. Transition loss curves for quartz sands of various shape factors. $C = 1000$ ppm by volume. ($o-C_s = 1.45$, $o-C_s = 1.55$, $+C_s = 1.65$.)



$$\pi d / \lambda$$

Fig. 6. Dimensionless attenuation of two metal powders covering part of all of the diffraction, transition, scattering and viscous loss ranges concentration = 1000 ppm by volume. (o-Tungsten $S_g = 18.9$, + Silicon $S_g = 2.4$.)

as $\pi d/\lambda$ decreases, and ft^2/ν is the correct abscissa for viscous loss—not $\pi d/\lambda$. The diffraction loss data is limited.

Conclusions

Experimental results of tests on a wide variety of natural sediments and metal powders for the various loss ranges are compared with the theoretical relations. For the viscous loss range, the empirical equation is an infinite natural log series the first term of which is nearly identical with the theoretical equation. The experimental data fits the natural log series considerably better than present theoretical equations. Experimental results yield only an apparent scattering loss equation because this range is short and the viscous loss is included in it for the smaller sizes. The slope of this line is a function of the relative density of the sediment and fluid. When the viscous attenuation is subtracted from the lower end of the apparent scattering loss equation, the slope of the scattering loss curve compares favorably with theory. The diffraction loss equation agrees in slope with theory when $\pi d/\lambda > 12.5$. When this range is defined for $\pi d/\lambda > 3.0$ a frequency dependence appears in the relations. Therefore, the upper boundary of the transition region between the diffraction and scattering loss ranges is set at $\pi d/\lambda = 12.5$.

The authors wish to acknowledge the financial support of the National Science Foundation in the form of Research Grant NSF G-971.

Literature Cited

- Anderson, V. C. 1950. Sound scattering from a fluid sphere. *Journal of the Acoustical Society of America*. 22:426-431.
- Busby, J., et al. 1955. The propagation of ultrasonic in suspensions of particles in a liquid. *Physical Society of London Proceedings*. 69:193-202.
- Carhart, R. S. 1950. Theory of viscous and thermal attenuation of sound by small spheres. Unpublished Ph.D. Dissertation, California Institute of Technology, Pasadena, California.
- Epstein, P. S. 1941. On the absorption of sound waves in suspensions and emulsions. Theodore Von Karman Anniversary Volume, California Institute of Technology, Pasadena, California.
- Faran, J. J. 1951. Sound scattering by solid cylinders and spheres. *Journal of the Acoustical Society of America*. 23:405-417.
- Flammer, G. H. 1958. The use of ultrasonics in the measurement of suspended sediment size distribution and concentration. Ph.D. Dissertation, University of Minnesota, Minneapolis, Minn.
- Killen, J. M. 1956. The measurement of sediment properties by the scattering of ultrasonic radiation in water. M.S. Thesis, University of Minnesota, Minneapolis, Minn.